UNIVERSITY OF TARTU
Faculty of Science and Technology
Institute of Technology

Paul Rihard Matute Perner

Flow cytometry analysis of extracellular vesicles.

Bachelor's Thesis (12 ECTS)

Curriculum Science and Technology

Supervisors:
PhD Reet Kurg
MSc Olavi Reinsalu

Tartu 2021

Flow cytometry analysis of extracellular vesicles.

Abstract:

Extracellular vesicles (EVs) are lipid-bound particles that are released by the cells into the extracellular space. However, the nature of EVs being small, make their analysis difficult. Flow cytometry is useful tool for analyzing a sample and its use for analyzing EVs is much desired. To overcome the size limitations, bead-assisted flow cytometry provides a mean for doing so. Yet, direct EV flow cytometry could potentially produce other reliable results that the nature of bead-assisted cannot. In this thesis, we studied four different samples by applying different analysis methods, followed by direct EV flow cytometry to determine whether it is possible to detect them via this method.

Keywords:

Flow cytometry, extracellular vesicles.

CERCS:

T490 Biotechnology

Ekstratsellulaarsete vesiikulite analüüs voolutsütomeetrilisel meetodil.

Lühikokkuvõte:

Ekstratsellulaarsed vesiikulid (EV) on lipiididega ümbritsetud osakesed, mida rakud sekrereteerivad rakuvälisesse ruumi. Kuna EV osakesed on väga väikesed, siis on nende analüüsimine raskendatud. Voolutsütomeetria on kasulik meetod, et analüüsida erinevad proove ja selle kasutamine EV de uurimisel väga soovitatav. Väikestest mõõtmetest tulenevaid raskusi on võimalik ületada kasutades helmestega assisteeritud voolutsütomeetria meetodit. Otsene EV voolutsütomeetria võimaldab saada täpsemaid kvantitatiivseid tulemusi, mida helmestega assisteeritud meetod ei suuda. Selles bakalauruse töös uuriti nelja erinevat proovi rakendades erinevaid analüüsimeetodeid ja seejärel otsest EV voolutsütomeetriat, et määratleda kas EVsid on võimalik sellel meetodil tuvastada.

Võtmesõnad:

Voolutsütomeetriat, Ekstratsellulaarsed vesiikulid

CERCS:

T490 Biotehnoloogia

TABLE OF CONTENTS

TERMS, ABBREVIATIONS AND NOTATIONS

EVs - Extracellular vesicles

MVB - Multivesicular bodies

MVs - Microvesicles

ESCRT - Endosomal sorting complex required for transport,

PBS - Phosphate buffered saline

MAGEA - Melanoma-associated antigen A

TBST - Tris-Buffered Saline, TWEEN 20

SDS-PAGE - Sodium dodecyl sulphate–polyacrylamide gel electrophoresis

PVDF- Polyvinylidene difluoride

EGFP - Enhanced Green Fluorescent Protein

GFP - Green fluorescent protein

mRNA - messenger RNA

miRNA - microRNA

INTRODUCTION

Extracellular vesicles are lipid-bound vesicles secreted by the cells. Evidence has shown that they provide a means for intercellular communication by the exchange of proteins, lipids, and genetic material. The growing evidence for the use of extracellular vesicles to identify different physiological and pathological conditions has portrayed a potential use as biomarkers in clinical settings. However, some knowledge in the field of extracellular vesicles is still unknown.

A major caveat in the field is the analysis of EVs. The innate size of extracellular vesicles limits the available detection methods. While attempting to increase the sensitivity of the methods, other issues begin to take place. This lead to disruptions in the data and further rendering some unreliability of the obtained results. Enhancements in these methods are much desired, as they would further improve the quality of the results and provide better studies overall.

The analysis of EVs by flow cytometry is no exception. Although research has overcome the size limitations by bead-assisted flow cytometry, the fact remains that direct EV flow cytometry is a much-desired method. By establishing a proper experiment environment while properly adjusting the instrument parameters, the detection and quantification of an EV-containing sample could potentially be reliable for research.

This thesis aims towards the characterization of an EV-containing sample directly by flow cytometry. By analyzing the results from other methods and theoretical knowledge, we can validate direct flow cytometry results and further arrive at educated conclusions from the obtained results.

1. LITERATURE REVIEW

1.1 Extracellular Vesicles

EVs are small membrane-enclosed particles derived from the cell membrane which are released through several pathways into the extracellular space. They were initially discovered as subcellular material from platelets and were termed *platelet dust* (Wolf 1967). These particles contain a cargo composed of mRNA, miRNA, proteins, and lipids (Deregibus, Cantaluppi et al. 2007) (Valadi, Ekstrom et al. 2007) (Ratajczak, Miekus et al. 2006) (Skog, Wurdinger et al. 2008) (Aliotta, Sanchez-Guijo et al. 2007) (Bacha, Blandinieres et al. 2018), and have shown to take roles in intercellular communication.

A recent interest in the study of EVs has surged and can be attributed to the fact that they provide a means for intercellular communication and transmission of macromolecules (Zaborowski, Balaj et al. 2015). EVs have also been demonstrated to be used as biomarkers for diagnostic purposes and have led to insight on cancer metastasis. Further research in the field of EVs may allow their use in clinical settings.

Nevertheless, the term extracellular vesicle is quite broad. The term refers to several subtypes of various sizes, functions, composition, and biogenesis. Yet, some basics of EVs biology are to be understood, and standardized methods for isolation and analysis are needed to improve the quality of the research.

1.2 Classification of EVs

As the field of EVs is still in development, definitions and classification are still lagging. Classification of EVs can be done regarding the size, density, biochemical composition, cell of origin, or other characteristics (Thery, Witwer et al. 2018). However, this has led to both overfitting and underfitting of the term and to the several EV subtypes.

The produced ambiguity is also enforced by the interchangeable use of EVs nomenclature (van der Pol, Boing et al. 2016), which presents irregularities for both the terminology and characterization of these particles among the scientific community.

For this literature review, we will be classifying extracellular vesicles into three main subtypes differentiated based upon their size, function, content, pathways, and biogenesis: microvesicles, exosomes, and apoptotic bodies (Zaborowski, Balaj et al. 2015).

1.2.1 Exosomes

Exosomes are generally in a size range of 40 - 100 nm and are formed from an endosomal route (Zaborowski, Balaj et al. 2015). Exosomes have been found in several biological fluids such as plasma (Caby, Lankar et al. 2005), urine (Pisitkun, Shen et al. 2004), saliva (Zlotogorski-Hurvitz, Dayan et al. 2015), breast milk (Admyre, Johansson et al. 2007), serum (Hornick, Huan et al. 2015), tears (Grigor'eva, Tamkovich et al. 2016), cereal spinal fluid (Akers, Ramakrishnan et al. 2013), synovial fluid (Li, Wang et al. 2018), bronchial fluid (Yuan, Bedi et al. 2018), lymph (Milasan, Tessandier et al. 2016), bile (Yoon and Chang 2017), gastric acid (Kagota, Taniguchi et al. 2019), amniotic fluid (Dixon, Sheller-Miller et al. 2018), and semen (Vojtech, Woo et al. 2014). As extracellular vesicles are expelled by every cell type, they provide a way for minimally invasive biopsy.

The formation of exosomes begins with the inward budding of early endosomes, which mature into multivesicular bodies. Later on, these MVBs are either sent to be degraded by a lysosome or can be fused unto the plasma membrane to be released with its content into the extracellular space, the latter being the release of exosomes (Bebelman, Smit et al. 2018). The factors determining the fate of MVB of either degrading or getting released as exosomes are yet to be understood (Raposo and Stoorvogel 2013); however, the MVB formation has been characterized to be done by two pathways: ESCRT-dependent and ESCRT-independent mechanisms.

On the ESCRT-dependent pathway, ESCRT-0 assembles with ubiquitinated proteins. ESCRT-0 is then incorporated into the endosomal membrane and recognized by ESCRT-I, which in turn passes ubiquitinated cargos. The assembly of the rest of the ESCRT machinery (ESCRT-II and ESCRT-III) clusters ubiquitinated cargo and induces a curvature of the endosomal membrane, which in turn form an intra-luminal vesicle (Wollert and Hurley 2010).

Despite some knowledge in the ESCRT-dependent pathway, the ESCRT-independent pathway is less understood. It is known that the system lacks some specificity as no cargo sorting occurs and that the resulting vesicle could contain an irregular set of endosomal membrane proteins (Babst 2011).

1.2.2 Microvesicles

Despite certain literature grouping microvesicles and exosomes together, microvesicles are instead formed by the direct outward budding of the plasma membrane followed by the fission of the plasma membrane. They present a noticeable broad spectrum of size ranging from 100 nm to 1000 nm.

The pathway for MV formation is yet to be fully understood. Regardless, it has been shown that the budding is mediated by coat proteins (Bonifacino and Lippincott-Schwartz 2003) which are recruited unto donor membranes and assembled by GTPases of the Arf1/Sar1 family. The coat proteins deform the membrane into buds while the cargo and fusion machinery are incorporated into the budding vesicle by binding to the coat subunits (Springer, Spang et al. 1999).

Enrichment of assorted lipids and proteins has been shown at the specific cell membrane locations where the shedding occurs. Cholesterol was shown to be a prevalent requirement for MV formation as the depletion of cellular cholesterol inhibited microvesicle shedding (Del Conde, Shrimpton et al. 2005).

EVs contain a high concentration of exposed phosphatidylserine in the outer leaflet. This aminophospholipid exposure suggests the inducing of morphological changes in the cellular membrane during MVs budding (Muralidharan-Chari, Clancy et al. 2010). This exposure has been shown to facilitate the internalization of MVs by recipient cells (Fitzner, Schnaars et al. 2011).

1.2.3 Apoptotic Bodies

Apoptotic bodies are released as a result of cell fragmentation during late apoptosis. Apoptotic bodies vary in size with a range of 50 nm up to 2000 nm. These membrane-bound vesicles are released into the extracellular space and are further removed by phagocytosis while avoiding an inflammatory response. The release of apoptotic bodies has been characterized in a wide range of cells and has become a feature of programmed cell death (Ihara, Yamamoto et al. 1998).

Although not yet fully understood, the formation of apoptotic bodies involves a physical process arising from the increased hydrostatic pressure and followed by actomyosin-mediated contraction (Charras, Yarrow et al. 2005). During the early stages of apoptotic

body formation, the blebs are lacking some cytoskeletal proteins. Shortly after, actin is polymerized within the structure and is followed by the recruitment of myosin and other cytoskeletal proteins that aid towards the retraction and expelling of the bleb (Charras, Hu et al. 2006).

Some findings have indicated apoptotic bodies taking important immune regulatory roles and being a possible means for intercellular communication (Holmgren, Szeles et al. 1999).

1.3 EVs Uptake and Communication

EV intracellular communication can occur via the interaction of the EV at the target cell surface without the inward budding (Raposo, Nijman et al. 1996) or by the internalization of the EV followed by either degradation or a re-release into the extracellular space (Luga, Zhang et al. 2012).

For uptake to occur, the acceptor cell requires compatibility of both the EVs' surface and its membrane. Docking would then occur through specific molecular interactions of proteins, lipids, or sugars situated across the membrane. Internalization of the EV would then happen by several reported mechanisms of phagocytosis and endocytosis, followed by the release of the EVs' contents (Abels and Breakefield 2016).

The mechanism for EV uptake depends on the cell type, physiologic state, receptors on the cell membrane, and ligands on the EVs' surface. Hence, several mechanisms for EV uptake have been described across the literature.

1.4 Methods for EV Isolation

Isolation, coupled with detection, remains the biggest challenge in EV research. An ideal EVs isolation would imply a high recovery yield with negligible physical and chemical damage and little contamination from other biomolecules or that of other extracellular vesicle subtypes. Regardless, current isolation protocols co-isolate cellular debris, exomeres, and different lipoproteins (Thery, Witwer et al. 2018).

The overlapping physical characteristics of the different EVs subtypes do not allow for individual isolation of each subtype (Mathieu, Martin-Jaular et al. 2019). Hence, isolation typically would involve an overlap of several subtypes.

1.4.1 Differential Centrifugation

Differential centrifugation is the most common method for EVs isolation. Several protocols for differential centrifugation exist and vary according to the experiments and sample needs but generally follow steps based on a B lymphocyte exosome extraction (Raposo, Nijman et al. 1996).

Differential centrifugation is done by separating the sample components in a stepwise manner (Revenfeld, Baek et al. 2014). While centrifuging, the larger components of the samples are moved away from the central axis, leaving the smaller components near the axis.

Hence, by using centrifugal force, contaminants of the samples containing the EVs can be removed and coupled by subsequent centrifugations, separation of different sizes of EVs can be achieved.

The general steps include the cell culture media or fluid sample being centrifuged to remove unnecessary cell components. This step is performed at low speeds for about 10-20 minutes and a low temperature, usually at 4 ºC (Revenfeld, Baek et al. 2014). The resulting supernatant is then centrifuged at a higher speed for usually longer times, keeping constant the temperature from the previous centrifugation. Proceeding centrifugations are performed to separate the content further. The extracted pellets of EVs are resuspended in PBS and stored at a low temperature of about -80 ºC for long-term storage (Momen-Heravi, Balaj et al. 2013). Still, storage at 4 ºC can be done for a short time frame storage.

No specific centrifugation speed determines the subtype of EV. Still, the recovery of the largest EVs is performed at around 2,000g for about 10-30 minutes of centrifugation. Meanwhile, for medium-sized EVs, centrifugation with a force of 10,000 - 20,000g for about 30 minutes leads to its recovery. In the case of the smaller EVs, centrifugation of much higher force (100,000 - 200,000g) and longer times must be performed (Mathieu, Martin-Jaular et al. 2019).

Even though differential centrifugation is the most common method for EVs isolation, the extracted sample's purity is questionable. These impurities are due to the aforementioned co-precipitation of cellular components, protein aggregates, and nucleosomal fragments (Momen-Heravi, Balaj et al. 2013).

1.4.2 Density Gradient Centrifugation

Separation still follows size and density; however, in density gradient centrifugation, the buoyant density is used to isolate EVs. The separation is achieved by centrifugation in the presence of a density gradient. Some commonly used solutions include sucrose and iodixanol. One clear advantage of density gradient centrifugation is the higher differentiation of the obtained products (Doyle and Wang 2019). However, the yield achieved is not high and requires a more extended preparation period (Zhang, Jin et al. 2018).

Density gradient centrifugation is typically performed after some previous differential centrifugation. The protocol roughly follows loading a tube with the desired solution with the partially isolated EVs sample dissolved in PBS and centrifuging such tube at high speed for an extended period. Afterward, partial transfer of the cushion/matrix to a new tube is then resuspended with PBS and centrifuged again (Thery, Amigorena et al. 2006).

1.4.3 Ultrafiltration

Ultrafiltration takes a size-based and molecular weight cut-off approach. EVs are isolated using membrane filters with pre-defined size limits. One problem arising from the filter is clogging. This clogging, in turn, results in a lower yield. Nevertheless, another problem is the deformation and lysis of EVs from the applied pressure to the sample (Li, Kaslan et al. 2017). Despite these drawbacks, the resulting purity is high (Zhang, Jin et al. 2018).

1.4.4 Immunoaffinity Capture

Immunoaffinity capture techniques use an antibody interaction with a specific protein in the EV surface. This methodology employs the antibodies getting fixed on magnetic beads, chromatography matrices, plates, or microfluidic devices (Thery, Amigorena et al. 2006).

One considerable advantage, or perhaps disadvantage, is the high specificity. If the intention is isolating specific subsets of marker positive EVs, this method does provide exemplary results. However, as expected, this method does not characterize the EV population of the sample as a whole. This limitation, paired with undefined markers for specific subtypes of EVs, does limit the situations this isolation method can be applied.

1.4.5 Precipitation

Precipitation is a method that uses a water excluding polymer. The principle is that the polymer binds to the water molecules, letting other sample particles precipitate. The resulting precipitated EV can then be pelleted for further analysis (Doyle and Wang 2019).

Despite seeming quite simple, it does have some significant drawbacks. For example, the co-precipitation of other proteins and materials results in a doubtful sample purity. On another point, it does limit the usage of the extracted EVs for significant results as the selectivity achieved is relatively low. However, coupling this method with some preliminary isolation could increase the quality of the extraction.

1.4.5 Microfluidic Technologies

Using the flow of liquids within small micro-sized channels, EVs are separated and trapped within the channels by some immunoaffinity properties (Carnino, Lee et al. 2019). These technologies have arisen to counter some of the limitations of other isolation techniques. Some advantages are quickness, high sample purity, and high binding efficiency. These benefits do seem to open up their applicability in clinical environments.

1.5 Analysis of EVs

1.5.1 Immunodetection

This analysis method is based upon the chemical and compositional properties of the extracellular vesicles. Such type of analysis relies on the recognition of antibodies to its antigen in the sample. The results indicate the presence or absence of marker proteins in the isolated EVs. The analysis can be performed via flow cytometry, western blotting, or other techniques that follow this detection strategy.

Flow cytometry using beads requires the isolation of EVs before the immobilization of the EVs onto the surface of the beads. Once the immobilization is done, the EVs in the beads are exposed to a fluorescent-coupled antibody. The beads are then passed through the laser of a flow cytometer, which records the emitted fluorescent signal (Doyle and Wang 2019).

Western blotting essentially follows the usual protocol. The isolated EVs are lysed, and the given proteins are denatured. The denatured proteins are then separated by SDS-PAGE and transferred to a membrane. The membrane is then filled with a blocking compound and followed by covering by a primary antibody and secondary antibody subsequently. Compared to other techniques, this method does allow for the detection of internal proteins in the EVs, as other techniques are limited to the content exposed on the surface of the EV.

1.5.2 Transmission Electron Microscopy (TEM)

By electron microscopy, a magnified image of the sample can be acquired from the directed electron beam. This tool has noteworthy qualitative and quantitative results in EV characterization (Linares, Tan et al. 2017).

1.5.3 Nanoparticles Tracking Analysis (NTA)

This method uses the Brownian motion to measure both the concentration and size distribution. Brownian motion dictates that lighter particles will diffuse faster and that the speed is relative to particle size. A laser beam is directed into the solution, and the mean velocity of the particles is measured and used to calculate the size of the particles (Carnino, Lee et al. 2019).

Problems arising from this method are not being able to differentiate between EVs and other particles while having size detection limits and several other constraints while characterizing a heterogeneous sample (Carnino, Lee et al. 2019).

1.5.4 Dynamic Light Scattering (DLS)

Using the same principle as in NTA, using a laser, the light scattering and intensities are detected and then analyzed to determine both size and distribution of particles inside the solution (Carnino, Lee et al. 2019).

1.6 Analysis of EVs by Flow Cytometry

A particular feature that limits the reliability of EV detection results is their inherent small size and dim signals produced. Most available methods lack the sensitivity and compensating for it, lead to results that could be considered unreliable due to data col-

lection of background artefacts or simply that of coincidence (Gorgens, Bremer et al. 2019).

Direct EV detection by flow cytometry can be done using a fluorescent-conjugated antibody. The fluid of EVs coupled with antibodies is channeled upon a focused stream that then passes through a beam that excites the sample's fluorescent proteins. Several sensors detect the arising scattered light.

Forward scatter is measured by either a photodiode or a photomultiplier tube placed directly in line with the laser beam's path. Side scatter is measured by a photomultiplier tube resulting from the dispersed particles after the beam contact with the sample. Fluorescence is detected from the redirection of the particles coming from the side scatter with a series of dichroic filters.

At this point, the trigger threshold comes into play. Out of the obtained signals, a distinction between the background and the sample must be made. Signals surpassing the threshold are recognizing as events, while the others are discarded.

However, on the smaller spectrum of EVs, the beam wavelength is often longer than that of the size of these smaller EVs, and the produced signal is lower than that of the background (Nolan and Duggan 2018). This renders the value for the lower end of the threshold to be severely limited. On top of that, sample background may arise from a residual dye, which further contributes to data noise on the lower end. These limitations make the direct detection of EVs to be tricky and uncertain.

An inherent problem of concentration characterization using flow cytometry is the "swarm effect". This effect can be characterized as the event where the detected signal is not characteristic of a single instance but that of cumulative cases at that particular event (van der Pol, van Gemert et al. 2012). Nevertheless, it can be plainly distinguished by running the samples at several dilutions. The resulting particle concentration and dilution factor should present a linear relationship. If the detected EVs are reduced at unexpected factors of that of the dilution, then the particular measurement experienced the effect. Therefore, it is ideal for performing the measurements at low concentrations.

An alternative method of flow cytometry uses the coupling of EVs into latex beads. This method provides a workaround for the resolution limit of direct EV detection. A

single bead will potentially bind several EVs. The fluorescent signal emitted from that particular bead will provide an adequate strong signal that can overcome the trigger threshold and distinguish itself from the background (Lof, Ebai et al. 2016).

2. AIM OF THE THESIS

The thesis aimed to investigate whether it's possible to analyze extracellular vesicles directly by flow cytometry. For such:

- MAGE-A4, CD63, and EGFP EVs were collected from mouse fibroblast cells.
- EVs were purified by differential centrifugation.
- The resulting samples were analyzed directly by flow cytometry utilizing two different approaches.

3. EXPERIMENTAL PART

3.1 MATERIAL AND METHODS

3.1.1 Cell Culture and Medium

The medium of COP5-EBNA, mouse fibroblast cells, was used for the experiment. For such, COP5-EBNA cells were cultured in IMDM medium supplemented with 10% fetal calf serum, penicillin (100 U/mL), and streptomycin (100 ng/mL) at 37 °C.

The cells were transfected with expression plasmids pEGFP or pQM-MAGEA4-EGFP or pQM-CD63-EGFP, mixed with 50 µg of salmon sperm carrier DNA, and then cultured in IMDM medium supplemented with 5% exosome free fetal calf serum, penicillin (100 U/mL), and streptomycin (100 ng/mL). For control, salmon sperm carrier DNA was used. Transfection was carried out at 230 V and 975 µF on the GenePulser Xcell™.

After electroporation, the medium was collected after leaving the cultures to grow for 72 hours. The resulting yield was about 40 mL for each cell culture.

3.1.2 Isolation of Extracellular Vesicles

Differential ultracentrifugation was the method implemented for the isolation of EVs. The protocol followed a paper published by Kurg Lab (Kuldkepp, Karakai et al. 2019). A general scheme of the ultracentrifugation steps is shown in Figure 1 and is further elaborated.

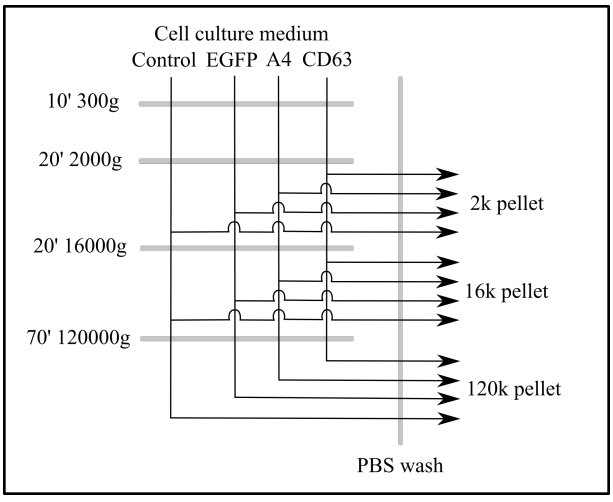

Figure 1. Scheme for isolation of EVs.

The medium was transferred directly from the cell culture dishes into 50 mL tubes. In order to remove cell debris from the medium, an initial centrifugation of 10 minutes at a force of 300g and a temperature of 4 ºC was performed using an Eppendorf 5810R centrifuge. The resulting supernatants were then transferred into new 50 mL tubes and were labelled *2k.*

The *2k* tubes were then centrifuged using the aforementioned centrifuge at a force of 2,000g for a duration of 20 minutes and at 4 ºC. The resulting supernatants were then transferred to new centrifugation tubes and labelled *16k.* The pellets from the *2k* tubes were resuspended in 100 µL of PBS.

Following, balancing the *16k* tubes was done using PBS and then loaded to the tubes of the SW28 rotor. Subsequently, centrifugation for the *16k* tubes, using the Ultima XE-90 ultracentrifuge, was performed for 20 minutes at a force of 16,000g and the same temperature. The resulting supernatants were then transferred to new centrifugation tubes and labelled *120k.* The pellets from the *16k* were then resuspended in 100 µL of PBS.

Tubes labelled *120k* were then balanced with PBS and loaded into the tubes of the same SW28 rotor. Subsequently, the tubes were centrifuged on the same centrifuge for 70 minutes at a force of 120,000g. Supernatants of the resulting *120k* tubes were discarded, and the pellets were resuspended in 3mL of PBS.

The *2k* and *16k* samples had 1400 µL of PBS added, followed by a resuspension. The samples were then transferred to Eppendorf tubes and centrifuged using Thermo Fisher's Scientific Fresco™ 17 Microcentrifuge with a force of 16,000g for 20 minutes and the same temperature of 4 ºC. The supernatants were carefully removed without disturbing the pellets and resuspended with 100 µL of PBS.

The *120k* samples were transferred to new centrifugation tubes. Balancing of the tubes was performed using PBS and loaded into the SW55 rotor. Centrifugation was performed at a force of 120,000g for 90 minutes and a temperature of 4 ºC on the Ultima XE-90 ultracentrifuge. The resulting supernatants were discarded, and the tubes were left to dry before resuspending in 100 µL of PBS.

All of the samples were stored in a cold room after isolation.

3.1.3 Bradford Assay.

In a 96-well plate, 4 µL of the following samples were added to two wells: H_2O, BSA protein standard for 0.1, 0.2, 0.4, 0.6, 0.8, and 1.0 mg/mL, and the *2k*, *16k*, *120k* samples.

Following, 200 µL of 1x Bio-Rad Protein Assay Dye Reagent was placed in each well. The optical density of the samples was then obtained using a parameter of 595 nm for wavelength absorbance. The protein concentrations of the samples were then calculated from the standard values.

3.1.4 Western Blot.

A quantity of 10 µL of the *2k*, *16k*, and *120k* samples were resuspended in 10 µL of Laemmli buffer and denatured for 10 minutes at a temperature of 100 ºC.

The samples were then separated electrophoretically in 10% SDS-PAGE gels. The volumes loaded into each well were calculated, accounting for the samples' protein concentration. In total, 3.80 µg of protein were loaded from each of the *120k* samples and a volume of 15 µL for both the *16k* and *2k* samples.

Following, semi-dry transfer was done onto a PVDF membrane using the Trans-Blot® SD Semi-Dry Transfer Cell from Bio-Rad. A voltage of 15 V for 25 minutes was used for this procedure.

The membrane was then blocked overnight with 5% non-fat dry milk in 20 mL of TBST [1xTBS and 0.1% Tween20].

After blocking, the solvent was discarded and replaced with 1% non-fat dry milk in 10 mL of TBST and 1 µL of anti-EGFP antibody. The PVDF membrane was left to incubate for 1 hour. The membrane was then washed three times using washing buffer [100 mM Tris-Cl, ph 7.5; 170 mM NaCl, 0.05% Tween20] for 10 minutes per wash.

Next, the membrane was placed with 1% non-fat dry milk in 10 mL of TBST and 1 µL of the secondary antibody and left to incubate for 1 hour. The membrane was then washed three times using washing buffer for 10 minutes per wash before acquiring the images by chemiluminescence techniques for darkroom development.

3.1.5 Direct EV Flow Cytometry

From the *120k* samples, 20 µg of EVs were taken and then diluted to 1:1000 in filtered PBS. Dilutions of 1:100 for the *16k* and *2k* samples were done.

Flow cytometry was performed on the samples using an Attune NxT Acoustic Focusing Cytometer. Gating was performed using 200 nm, 500 nm, and 1000 nm FACS calibration beads.

Two different optical filters were used for flow cytometry. Total events recorded are from a constant volume draw of 50 µL with a flow rate of 12.5 µL/minute. Two rinses were performed after every reading to ensure no cross-sample readings. The following parameters were used:

488/10+002.

Voltage: FSC 500, SSC 370, BL1 450
Threshold: SSC 0.2 AND BL1 0.2
Width threshold setting: 1
Area scaling factor: Blue 0.7

488/10.

Voltage: FSC 300, SSC 235, BL1 420
Threshold: SSC 0.2 AND BL1 0.2
Width threshold setting: 1
Area scaling factor: Blue 0.7

3.1.6 Bead-Assisted Flow Cytometry

Protocol for this method is based on that of the same paper that differential centrifugation was based upon (Kuldkepp, Karakai et al. 2019).

A single drop of 4 µm diameter aldehyde/sulphate latex beads were mixed with 20 µg of the *120k* samples in 1000 µL of PBS. Samples were incubated overnight in a rotator. Following, samples were centrifuged and resuspended in new PBS. The same flow cytometer, as in the direct EV flow cytometry, was used. Data was acquired from ~30,000 bead events.

The following parameters were used:

Voltage: FSC 350, SSC 350, BL1 440

Threshold: OR FSC 25

Width threshold setting: 1

Area scaling factor: Blue 1.23

3.2 ANALYSIS OF EXTRACELLULAR VESICLES

3.2.1 Bradford Assay

As previously stated in the methods section, the samples were control, EGFP, CD63-EGFP, and MAGE-A4-EGFP. For simplicity reasons, MAGE-A4-EGFP sample will be called A4 and CD63-EGFP as CD63.

After isolation by differential centrifugation, the protein concentration of the extracted EV samples was obtained to use in further calculations. Regardless, the result confirmed the isolation of material from the cell culture medium.

The concentration for the *120k* samples was in the expected ranges (Table 1). However, the resulting concentrations for both the *16k* and *2k* samples were on the lower end, with the *16k* samples presenting particularly low numbers (Table 2).

Table 1. Protein concentration of the *120k* samples from Bradford Assay analysis.

Sample	Concentration (μg/μL)
Control	0.237
EGFP	0.312
A4	0.365
CD63	0.419

From 40 mL of medium

Table 2. Protein concentration of the *16k* and *2k* samples obtained from Bradford Assay analysis.

Sample	16k Concentration (μg/μL)	2k Concentration (μg/μL)
Control	0.009	0.222
EGFP	-0.010	0.046
A4	0.083	0.065
CD63	0.013	0.019

From 40 mL of medium

As for the *2k* samples, the concentration of the control sample was higher overall. Being the samples resulting from the first centrifugation, the co-isolation of some other cellular components that were not initially removed, was expected.

3.2.2 Western Blot

To determine whether the isolated EVs contained the protein with the EGFP coupled molecule, western blotting was performed.

From the theoretical background, a band for control should not be present. In the same way, the same scenario for the EGFP sample must also hold. This scenario is since EGFP usually is to be found in the cytoplasm. Therefore, it should not get included in extracellular vesicles of any size. The resulting western blot image did validate these predictions by not showing a band (Figure 2).

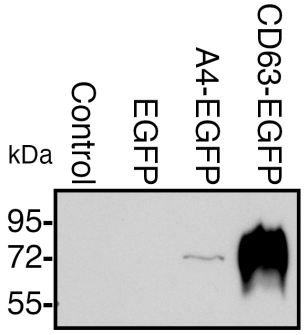

Figure 2. Western blot analysis *120k* samples. Analysis was performed with EGFP specific antibodies. Image was acquired after 15 minute exposure.

In another matter, it was expected for both A4 and CD63 in the *120k* samples to show a band. The assumption was correct and was visually represented by its corresponding western blot image.

Moreover, the expression intensity for CD63 was well above that of the A4 sample. This finding indicated higher incorporation of CD63 into extracellular vesicles.

As for the *16k* and *2k* samples, both control and EGFP were expected not to present a band. This characteristic did prevail in the experiment (Complementary Figure 1). The *16k* samples for A4 and CD63 also showed a dimmer band; however, the bands in their *2k* counterpart were extremely faint.

3.2.3 Bead-Assisted Flow Cytometry.

Bead-assisted flow cytometry for EVs analysis is a well-explored technique. On that account, this method was performed with the *120k* samples to examine the properties of the isolated EVs (Figure 3).

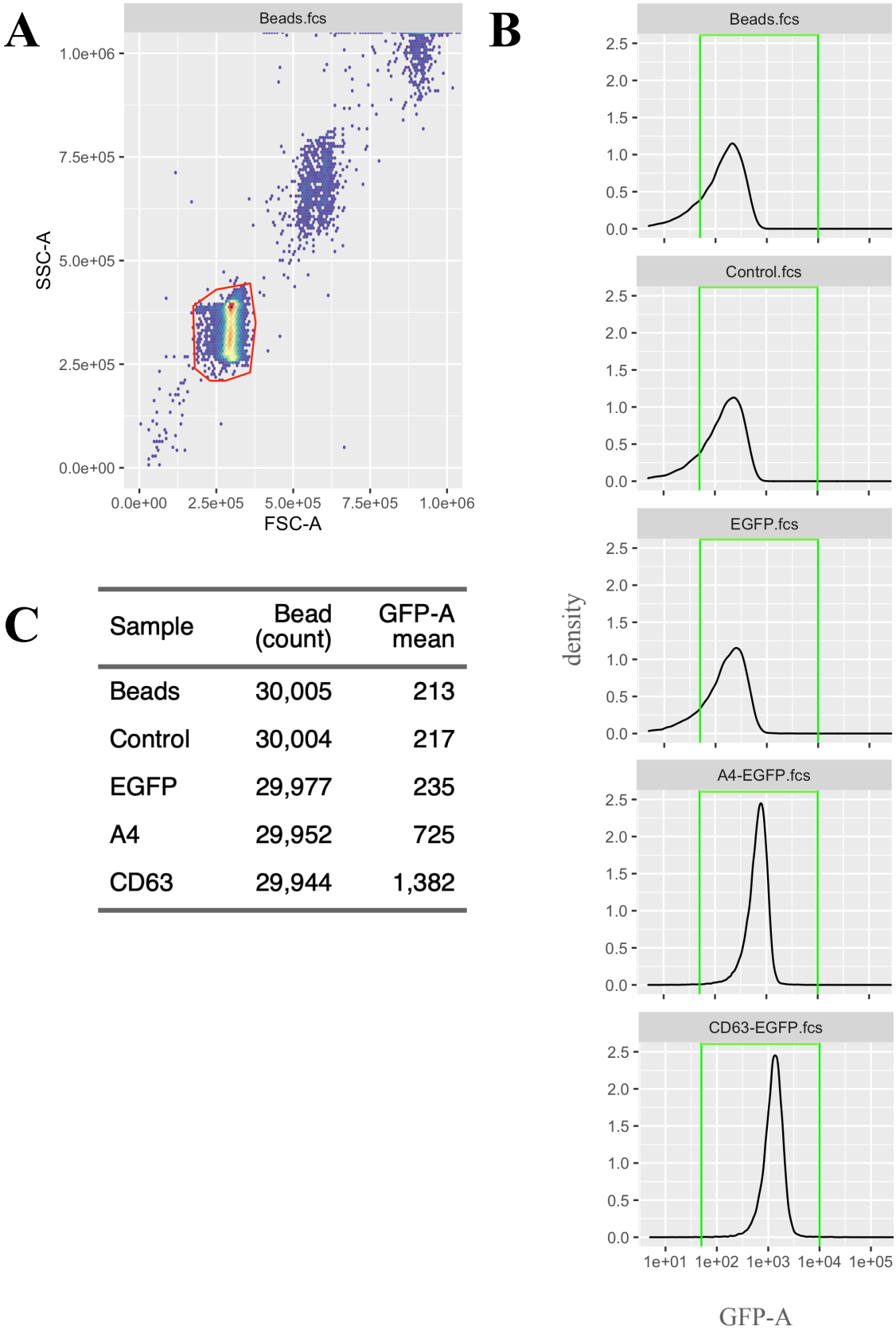

C

Sample	Bead (count)	GFP-A mean
Beads	30,005	213
Control	30,004	217
EGFP	29,977	235
A4	29,952	725
CD63	29,944	1,382

Figure 3. Results from bead-assisted flow cytometry. **(A)** Dot plot of bead-only sample with a red gate for single bead events. **(B)** Density plot of single bead readings with GFP positive gate shown in green. **(C)** Table showing count and GFP-A mean for the gated readings.

A bead-only sample was used as a reference for the analysis of the samples. The relative size of the beads being depicted by the forward scatter and the internal complexity by the side scatter is indeed a discernible point of reference for studying the samples.

For the experiment, three distinct populations were seen diagonally in the dot plots (Figure 3A). These points were characterized as single beads, double bead, and triple bead event readings. For study purposes, data was only acquired from the single beads events with an additional gate for GFP-A, which further characterized single bead events expressing GFP positive (Figure 3B).

The resulting GFP-A mean for the beads, control, and EGFP samples did not present a significant difference amongst them (Figure 3C). The numbers implied that similar characteristics were bound to these three samples.

To further elaborate, the baseline value for GFP was determined by the bead-only sample. Control, as determined by the sample's own nature, does not have any EGFP and therefore not present any GFP emission. As for the EGFP sample, it was determined by western blot that it does not get incorporated into EVs. Following that, it should not present discernible differences from both the control and the bead-only sample.

As for A4 and CD63, the GFP-A mean was much higher than with other samples, entailing that these markers were indeed incorporating into extracellular vesicles. Moreover, these two samples also presented a dissimilarity among themselves as the GFP-A mean of CD63 was higher. The same observation was also explicitly seen from the western blot experiment, as the CD63 sample had a more intense band in the image and therefore suggested that CD63 is more likely to be incorporated into extracellular vesicles.

The results obtained from bead-assisted flow cytometry, although able to characterize the sample, do limit the observed results. Each of the bead events presented a recorded instance of a conglomerate of EVs and not that of a single EV, essentially showing grouped characteristics instead of singular data.

In a similar matter, some other relevant information, such as the size of the particles, is obstructed and cannot be obtained with this particular method.

3.2.4 Direct EV Flow Cytometry

The approach of using direct EV flow cytometry was enticed by the aforementioned assertion. However, the caveat of direct EV flow cytometry is the method's own limitations. Detection of small particles by flow cytometry encompassed an increase in the instrument sensibility. This increase, however, aggregated to the noise levels arising from the sample solvents. Tuning of parameters in order to reduce this noise while still characterizing factual events, is a major challenge for small particle analysis.

For characterizing the contents of the samples directly, two different experiment environments were established with two different optical filters: 488/10 +002 and Attune™ NxT Small Particle Side-Scatter Filter, following the naming convention of Filter A and B, respectively. Characterization of positive events was based on the fluorescent values in the blue channel, which recorded for GFP emission.

Regardless of the optical filter used, background noise from the sample solvent is unavoidable when detecting particles at this lower size range. Therefore, the obtained data was based on setting the solvent readings as the baseline for calculations. For such, PBS readings were obtained with these two experiment environments.

The number of events from the PBS samples showed a steep decline for the <200 nm size with the filter B (Complementary Table 1). This decline suggested that this filter could provide better results for the lower-sized events, as potentially, fewer false-positive events could occur during the readings of the other samples.

As for the samples' readings, in order to achieve an adequate comparison environment, the same volume draw was used as well as the lowest possible flow rate. Furthermore, the collected data was obtained using large volumes intakes to mitigate the variability that sudden irregular events could generate and, in turn, produce a shift of the data towards incidental results. Lastly, to gain more confidence in our data, the mean of three round of readings were utilized for each sample.

To further evaluate the fluorescent expression of the sample, gating of GFP positive events was done from the PBS readings of each filter.

The percentage of GFP positive for all the *120k* samples using filter B was below the other filter (Table 3). This reduction suggested that the use of filter B leads to a lower number of false-positive events and that it might provide better results overall.

Table 3. Percentage of GFP positive events in the *120k* samples.

120k	Control		EGFP		A4		CD63	
Filter	A	B	A	B	A	B	A	B
GFP positive %	0.16%	0.00%	6.36%	1.21%	10.37%	2.70%	15.89%	4.47%

As to the comparison between these reading to that of bead-assisted flow cytometry, the percentage of GFP positive showed a strong correlation concerning the general characteristics of the samples. In a few words, barely to no GFP expression in control and EGFP, and more prominent expression for CD63 than for A4.

To further elaborate, control measurements with filter B, and to a lesser extent filter A, showed practically no GFP positive events. These results were the expected outcome from the assumptions that were drawn from the bead-assisted results. This result also supported the supposition of fewer false positives when utilizing filter B. The results of the EGFP sample did also collaborated with this, as the same outcome was obtained.

Following, it was previously seen during bead-assisted flow cytometry and western blot that the GFP intensity from that CD63 was higher than in the A4 sample. Direct flow cytometry did indeed show congruity by having a higher percentage of GFP positive events with CD63 than with A4.

Given the results, the comparison of the *120k* samples from the other experiments to the numbers of direct flow cytometry showed striking resemblance and indicated successful direct EV detection.

Taking into account the *16k* and *2k* samples, these samples maintained similarities to the *120k* results (Complementary Table 3). The lower percentage of positive events was also maintained with the readings from filter B.

However, there was a noticeable higher value with the EGFP samples. Three possible reasons could explain this outcome. The first reason assumes that these values are factual and that EGFP was incorporated into the EVs. The second reason would be the innate fluorescence emission from particles; however, control values indicated that this was not the case within the experiment's environment. The third reason would be the co-isolation of EGFP protein that might have been found from the initial medium. Moreover, a combination of the first and third reasons is also in the realm of possibility.

In a follow-up note, visual analysis of the dot plots of the samples showed some distinct subpopulations of EVs. A more distinguishable example from the *120k* samples was with CD63 (Figure 4). A conglomerate of EVs was visually appreciated with a diagonal-like distribution. Although already established, this visual characterization provided an example that the readings represent EVs, not that of just some random incidental events.

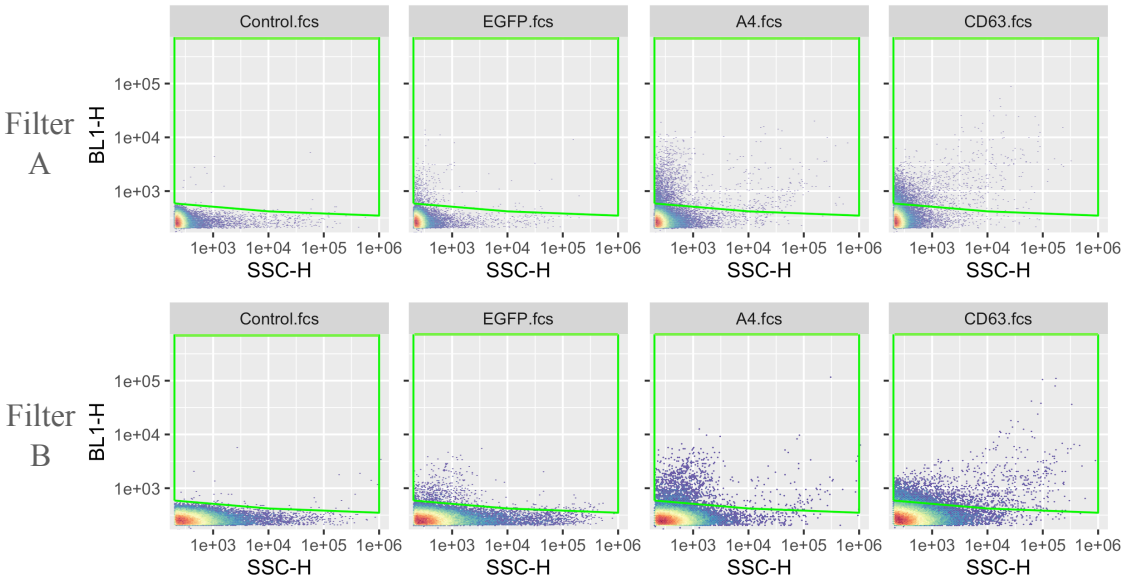

Figure 4. Direct EV flow cytometry of the *120k* samples. Dot-plot of the samples is shown with side scatter in the x-axis, and BL1-H in the y-axis. A GFP positive gate is shown in green. First row and second row show results with filter A and filter B, respectively.

Interestingly, *2k* samples contained subpopulations of EVs that were not particularly seen with the *16k* samples on the >1000 nm size (Figure 5 and 6). These subpopulations corresponded to apoptotic bodies. Hence, differential centrifugation is a method that does indeed isolate, although not perfectly, in a size-based manner.

Other subpopulations of EVs in the *16k* samples can also be visually identified (Figure 6). Moreover, their location appeared shifted towards the lower ranges than on the *2k*, further proving the effectiveness of size-based isolation via differential centrifugation.

To further characterize these visual properties in a number-based approach, events were extracted from the GFP positive gates and proceeded by size gating (Complementary Figure 2). The size gating was performed with calibration beads of 200, 500, and 1000 nm.

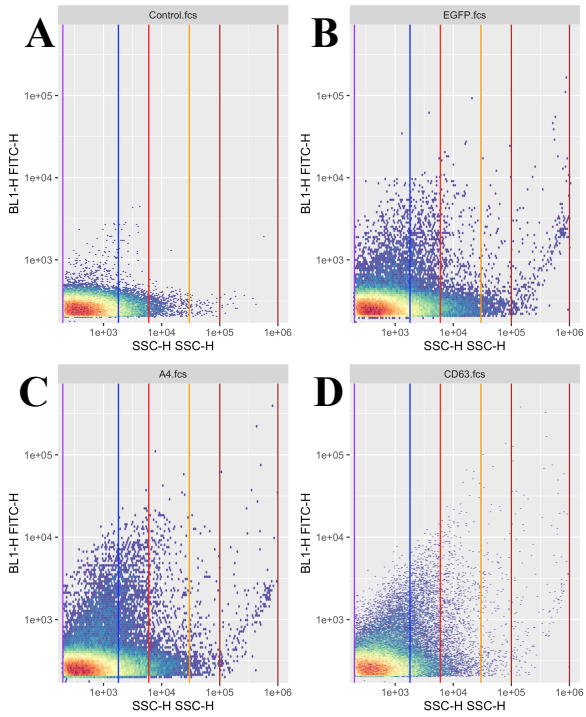

Figure 5. Direct flow cytometry of the *2k* samples using filter B. Dot-plots of with size gates for **(A)** control, **(B)** EGFP, **(C)** A4, and **(D)** CD63. Gate showing from leftmost quadrant <200, 200-350, 350-750, 750-1000 and >1000 nm particles.

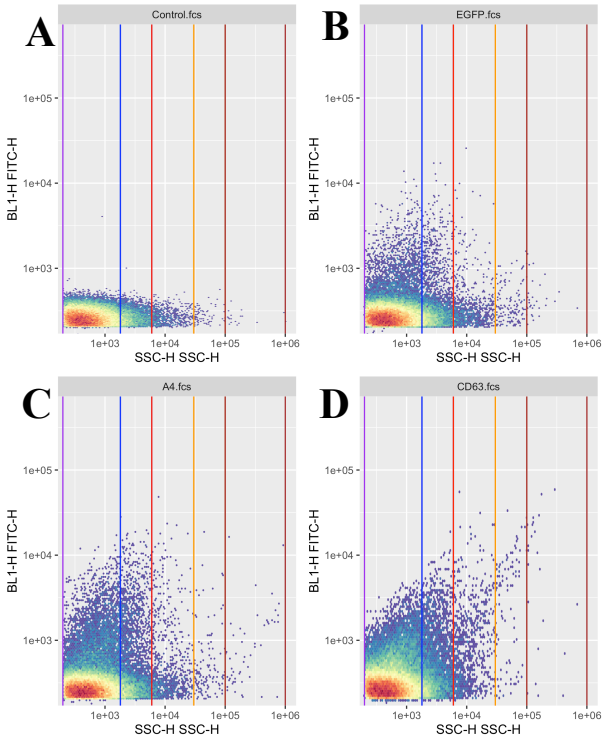

Figure 6. Direct flow cytometry of the *16k* samples using filter B. Dot-plots of with size gates for **(A)** control, **(B)** EGFP, **(C)** A4, and **(D)** CD63. Gate showing from left-most quadrant <200, 200-350, 350-750, 750-1000 and >1000 nm particles.

A higher percentage of events in the <200 for *120k* than in *2k* and *16k* were seen. These higher numbers collaborated to the effectiveness of differential centrifugation, dividing the sample by size (Figure 7). However, it also showed that co-isolation of some small fluorescent emitting particles was happening with the *2k* samples.

On another note, it was appreciated for a significantly higher percentage of positive events on the smaller sizes for each of the *120k* samples (Complementary Table 4). This increase suggested that the obtained *120k* centrifugation samples could have a higher purity when utilizing the used isolation method.

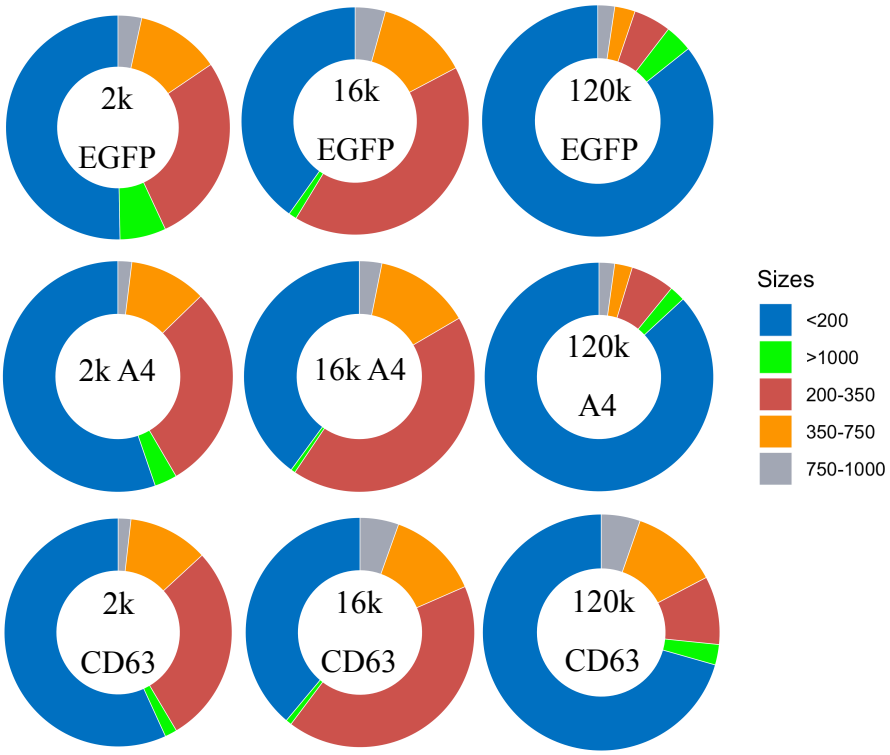

Figure 7. Pie charts showing the size distribution of GFP positive events.

As for the *16k* samples, from the reference frame of its *120k* counterpart, its events were reduced for the <200 nm particles and distributed towards larger sizes. Therefore, it indicated that the *16k* samples contain a more considerable amount of microvesicles and proved the visual remarks regarding the location shift in the subpopulations.

Continuing, CD63 is characterized chiefly as an exosome marker, meaning that it should, for the most part, be included in the lower size range. This property was actually seen in the experiment as the *120k* sample for CD63 did present most of its events in the lower ranges.

It was also qualified, for that matter, that A4 gets incorporated to the lower size particles as the number of positive events is significantly distributed to the lower end of the *120k* samples.

3.3 DISCUSSION

Favorable results were seen during the experimental part. Having accomplished a numerical characterization of the samples that did resemble the theoretical aspects of itself and followed the observations of the other characterizing methods, was a good indicator that direct EV flow cytometry could have further applications in other research experiments.

Regarding the results of direct EV flow cytometry, it was possible to confirm some knowledge about EVs. These reaffirmations were due to having had characterized some properties regarding the markers used. In a follow-up note, it was as well possible to describe the isolation result of differential centrifugation.

For the experiments, three different proteins incorporated into extracellular vesicles were analyzed.

CD63 is known to be a marker for exosomes and is commonly used for EV detection (Campos-Silva, C., et al. 2019). It is not only involved in the analysis but also used for immunocapture of EVs and enrichment along with other tetraspanins such as CD9 and CD81. As its incorporation into EVs is predominant, it is a suitable marker for research. In the case of this thesis, its usage was essential for verifying results and analyzing the outcomes of the utilized techniques.

Another marker used was A4. This marker belongs to a family of tumor-associated antigens. It was shown that this protein gets incorporated into EVs and is released by COP5-EBNA when expressed within these cells (Kuldkepp, Karakai et al. 2019). As cancer cells secret more EVs, this increased amount, plus the packaging of cancer-related molecules, shows promise towards EV-based cancer diagnosis.

Lastly, EGFP as a sole protein was able to give us remarks about its integration into EV. Also, as it does not get, for the most part, incorporated into EVs, it indirectly served as a control sample. In another aspect, it also provided a way to qualify the isolation procedure.

As the purpose of this thesis was to analyze EVs, coupling CD63 and A4 with a reporter protein, such as EGFP, made it possible to obtain values regarding the specific marker. During the western blot experiment, the detection of EGFP content was the desired outcome, while during flow cytometry, the emitted fluorescence of EGFP.

During direct flow cytometry, two different approaches were taken. As previously stated, the main difference were the optical filters used; filter A, which was a 488/10 +002 filter, and filter B, which was the Attune™ NxT Small Particle Side-Scatter Filter.

Both the filters comprise a band-pass functionality, allowing for the transmission of the wavelengths in the 483 to 493 nm range. These wavelengths correspond to the light spectrum for blue light and were therefore needed during the experiment.

The main difference is that filter A has an additional OD 2 filter lens. This lens limits the light able to pass through and lowers the transmission at the specific spectrum. From such, filter B could provide an enhanced performance when detecting small particles.

To stipulate whether the performance was better with filter B than A, the obtained numbers from the control sample provided insight and showed that, indeed, filter B was better. On another note, the experiments done in this thesis did not use ultra-filtered focusing fluid, which could have potentially enhanced the results, provided a decrease in background noise.

To clear a remark, as indicated by the filter specifications, the performance of this filter for larger-sized particles decreases as it would provide a saturated signal. So it is necessary to contemplate this performance aspect if used for any other type of experiment.

Taken all into consideration, robust methods for direct EV flow cytometry are still something to strive for. As experimentally seen in this thesis, even small changes did provide distinct results. Moreover, these differences could even be potentially produced by different instruments. All this together limits its application for high throughput screening.

Additionally, the innate nature of the samples' solvent does collide with the detection of extracellular vesicles and might lead to some inaccuracies. Furthermore, no distinction between EVs and some other cellular components can be entirely made with the current method. Yet, another distinction that cannot be made is from the noise arising from the own components of the flow cytometer. These problems entitle the use of precaution and thorough analysis when drawing conclusions from the results.

In addition, very proper experiment conditions must be met to get meaningful and confident data, making direct EV flow cytometry a time-consuming method that requires rigorous and thorough preparation.

Proceeding with the experiment results, western blot showed that EGFP does not incorporate into EVs. In more of a follow-up, it entails that it is a cytosolic protein. On the matter of CD63 and A4, it was affirmed that both of them are incorporated into extracellular vesicles. More so, CD63 expressed higher intensity, further proving that it is prominently integrated into EVs and is definitely an EV marker.

Following with bead-assisted flow cytometry, the same outcomes of integration into EVs were seen. The prominent integration of CD63 into EVs was as well seen by the higher expression. As for A4, its fluorescent expression was lower than CD63 but at well-found levels. In summary, western blot and bead-assisted flow cytometry indicated the same outcomes.

As to the results of direct EV flow cytometry, it was validated that the readings were of the EVs by having similar properties. Moreover, it was determined from the control samples that filter B gave a better performance as it reduced the number of positive events.

By having utilized calibration beads of different sizes, it was possible to characterize the samples further. To elaborate on the importance of differentiating the sizes, it allows for the distinction of EVs subtypes. Smaller sizes EVs usually encompass exosomes and are primarily found in the <200 nm range. Although having a broad and overlapping size range, microvesicles are larger than exosomes and are typically found between the 200 nm to 1000 nm range. Meanwhile, larger EVs and apoptotic bodies are mainly on the upper-sized spectrum at the >1000 nm range.

With this division by size, direct EV flow cytometry results also gave remarks about the isolation method. In particular, it showed better isolation for the *120k* samples with a more extensive distribution of positive events in the lower size range. Another noticeable result was the high co-isolation of particles from the *2k* samples. It also indicated that *16k* samples contained larger particles than the *120k* sample.

Into more of the markers, the results reaffirmed that CD63 is an exosome marker based on the size properties. Alas, from the approach taken within this experiment, the same cannot be confidently said from a biogenesis standpoint and does require validation from other experiments. Nevertheless, it was seen that A4 is more likely to be incorpo-

rated into exosomes. However, the same logic of CD63 applies and cannot be affirmed from a biogenesis standpoint.

To add to the relevance of direct EV flow cytometry, a convenient and expressed usage within this thesis, was the distinction of EVs by their size. This distinction cannot be seen with bead-assisted flow cytometry as the results only pertained to that of the conglomerate of EVs in the beads. This further aids the cause of improving direct EV flow cytometry.

Even more so, the results of bead-assisted flow cytometry showed little to no clear distinction inside the readings. Drawing meaningful information from the fluorescent intensities of the events did not convey much and almost rendered its results to binary outcomes.

Western blot techniques for the study of EVs do have their merit. The bands presented from the developed images did characterize the specific marker of research and its molecular weight. Furthermore, it also expressed the amount of protein present. Hence, its use for EV characterization is most valuable, and its importance should not be easily dismissed.

In that regard, the coupling of methods for EV analysis is essential for a throughout experiment. The results collaborated significantly towards the drawing of conclusions and asserted our finding from direct EV flow cytometry.

On that note, future experiments for direct EV flow cytometry must have very proper controls and protocols. Otherwise, the finding could be characterized as incidental. As standardized protocols are not yet established, one should be wary of the methodology used in the literature. Hopefully, future enhancements for this technique will facilitate the experimental part and focus research towards new findings rather than deal with the methodology.

In conclusion, the analysis of direct EV flow cytometry does have many challenges, but it is possible to mitigate them by taking the proper measures. The use of other techniques does contribute with helpful information, and coupling these observations, provides a more thorough characterization. The improvement of current methods will significantly improve the quality of the obtained results and collaborate to its potential use for diagnostic purposes.

SUMMARY

Extracellular vesicles (EVs) are lipid-bound particles that are released into the extracellular space. They provide a means for extracellular communication; however, they are particularly small, resulting in some limitations for their study.

Flow cytometry is a method that provides quantifiable results for a sample. In this regard, analyzing EVs by utilizing flow cytometry is an appealing method. However, the innate size of EVs is a severely limiting factor. Current research has overcome this restrain by doing bead-assisted flow cytometry; however, the resulting data becomes characteristic of a conglomerate of extracellular vesicles bind to a bead and not that of a singular EV in the sample.

The aim of the thesis was to characterize an EV-containing sample directly by flow cytometry. By setting up the experiment environment for increased sensitivity, including baseline numbers for calculation and optimizing the parameters, proper data was acquired that characterized the sample. Accordingly, by comparing the results obtained from other methods, informed conclusions were drawn.

REFERENCES

Abels, E. R. and X. O. Breakefield (2016). "Introduction to Extracellular Vesicles: Biogenesis, RNA Cargo Selection, Content, Release, and Uptake." Cell Mol Neurobiol 36(3): 301-312.

Admyre, C., et al. (2007). "Exosomes with immune modulatory features are present in human breast milk." Journal of Immunology 179(3): 1969-1978.

Akers, J. C., et al. (2013). "MiR-21 in the extracellular vesicles (EVs) of cerebrospinal fluid (CSF): a platform for glioblastoma biomarker development." PLoS One 8(10): e78115.

Aliotta, J. M., et al. (2007). "Alteration of marrow cell gene expression, protein production, and engraftment into lung by lung-derived microvesicles: A novel mechanism for phenotype modulation." Stem Cells 25(9): 2245-2256.

Arraud, N., et al. (2016). "Fluorescence triggering: A general strategy for enumerating and phenotyping extracellular vesicles by flow cytometry." Cytometry A 89(2): 184-195.

Babst, M. (2011). "MVB vesicle formation: ESCRT-dependent, ESCRT-independent and everything in between." Curr Opin Cell Biol 23(4): 452-457.

Bacha, N. C., et al. (2018). "Endothelial Microparticles are Associated to Pathogenesis of Idiopathic Pulmonary Fibrosis." Stem Cell Reviews and Reports 14(2): 223-235.

Bebelman, M. P., et al. (2018). "Biogenesis and function of extracellular vesicles in cancer." Pharmacol Ther 188: 1-11.

Bonifacino, J. S. and J. Lippincott-Schwartz (2003). "Coat proteins: shaping membrane transport." Nat Rev Mol Cell Biol 4(5): 409-414.

Caby, M. P., et al. (2005). "Exosomal-like vesicles are present in human blood plasma." Int Immunol 17(7): 879-887.

Campos-Silva, C., et al. (2019). "High sensitivity detection of extracellular vesicles immune-captured from urine by conventional flow cytometry". Sci Rep 9, 2042.

Carnino, J. M., et al. (2019). "Isolation and characterization of extracellular vesicles from Broncho-alveolar lavage fluid: a review and comparison of different methods." Respir Res 20(1): 240.

Charras, G. T., et al. (2006). "Reassembly of contractile actin cortex in cell blebs." J Cell Biol 175(3): 477-490.

Charras, G. T., et al. (2005). "Non-equilibration of hydrostatic pressure in blebbing cells." Nature 435(7040): 365-369.

Del Conde, I., et al. (2005). "Tissue-factor-bearing microvesicles arise from lipid rafts and fuse with activated platelets to initiate coagulation." Blood 106(5): 1604-1611.

Deregibus, M. C., et al. (2007). "Endothelial progenitor cell-derived microvesicles activate an angiogenic program in endothelial cells by a horizontal transfer of mRNA." Blood 110(7): 2440-2448.

Dixon, C. L., et al. (2018). "Amniotic Fluid Exosome Proteomic Profile Exhibits Unique Pathways of Term and Preterm Labor." Endocrinology 159(5): 2229-2240.

Doyle, L. M. and M. Z. Wang (2019). "Overview of Extracellular Vesicles, Their Origin, Composition, Purpose, and Methods for Exosome Isolation and Analysis." Cells 8(7).

Fitzner, D., et al. (2011). "Selective transfer of exosomes from oligodendrocytes to microglia by macropinocytosis." J Cell Sci 124(Pt 3): 447-458.

Gorgens, A., et al. (2019). "Optimisation of imaging flow cytometry for the analysis of single extracellular vesicles by using fluorescence-tagged vesicles as biological reference material." J Extracell Vesicles 8(1): 1587567.

Grigor'eva, A. E., et al. (2016). "Characteristics of exosomes and microparticles discovered in human tears." Biomed Khim 62(1): 99-106.

Holmgren, L., et al. (1999). "Horizontal transfer of DNA by the uptake of apoptotic bodies." Blood 93(11): 3956-3963.

Hornick, N. I., et al. (2015). "Serum Exosome MicroRNA as a Minimally-Invasive Early Biomarker of AML." Sci Rep 5: 11295.

Ihara, T., et al. (1998). "The process of ultrastructural changes from nuclei to apoptotic body." Virchows Arch 433(5): 443-447.

Kagota, S., et al. (2019). "Analysis of Extracellular Vesicles in Gastric Juice from Gastric Cancer Patients." Int J Mol Sci 20(4).

Kuldkepp, Anneli et al. (2019). “Cancer-testis antigens MAGEA proteins are incorporated into extracellular vesicles released by cells.” Oncotarget 10(38): 3694-3708.

Li, P., et al. (2017). "Progress in Exosome Isolation Techniques." Theranostics 7(3): 789-804.

Li, Z., et al. (2018). "Emerging Role of Exosomes in the Joint Diseases." Cell Physiol Biochem 47(5): 2008-2017.

Linares, R., et al. (2017). "Imaging and Quantification of Extracellular Vesicles by Transmission Electron Microscopy." Methods Mol Biol 1545: 43-54.

Lof, L., et al. (2016). "Detecting individual extracellular vesicles using a multicolor in situ proximity ligation assay with flow cytometric readout." Scientific Reports 6.

Luga, V., et al. (2012). "Exosomes mediate stromal mobilization of autocrine Wnt-PCP signaling in breast cancer cell migration." Cell 151(7): 1542-1556.

Mathieu, M., et al. (2019). "Specificities of secretion and uptake of exosomes and other extracellular vesicles for cell-to-cell communication." Nat Cell Biol 21(1): 9-17.

Milasan, A., et al. (2016). "Extracellular vesicles are present in mouse lymph and their level differs in atherosclerosis." J Extracell Vesicles 5: 31427.

Momen-Heravi, F., et al. (2013). "Current methods for the isolation of extracellular vesicles." Biol Chem 394(10): 1253-1262.

Muralidharan-Chari, V., et al. (2010). "Microvesicles: mediators of extracellular communication during cancer progression." J Cell Sci 123(Pt 10): 1603-1611.

Nolan, J. P. (2015). "Flow Cytometry of Extracellular Vesicles: Potential, Pitfalls, and Prospects." Curr Protoc Cytom 73: 13 14 11-13 14 16.

Nolan, J. P. and E. Duggan (2018). "Analysis of Individual Extracellular Vesicles by Flow Cytometry." Methods Mol Biol 1678: 79-92.

Pisitkun, T., et al. (2004). "Identification and proteomic profiling of exosomes in human urine." Proc Natl Acad Sci U S A 101(36): 13368-13373.

Raposo, G., et al. (1996). "B lymphocytes secrete antigen-presenting vesicles." J Exp Med 183(3): 1161-1172.

Raposo, G. and W. Stoorvogel (2013). "Extracellular vesicles: exosomes, microvesicles, and friends." J Cell Biol 200(4): 373-383.

Ratajczak, J., et al. (2006). "Embryonic stem cell-derived microvesicles reprogram hematopoietic progenitors: evidence for horizontal transfer of mRNA and protein delivery." Leukemia 20(5): 847-856.

Revenfeld, A. L., et al. (2014). "Diagnostic and prognostic potential of extracellular vesicles in peripheral blood." Clin Ther 36(6): 830-846.

Skog, J., et al. (2008). "Glioblastoma microvesicles transport RNA and proteins that promote tumour growth and provide diagnostic biomarkers." Nature Cell Biology 10(12): 1470-U1209.

Springer, S., et al. (1999). "A primer on vesicle budding." Cell 97(2): 145-148.

Thery, C., et al. (2006). "Isolation and characterization of exosomes from cell culture supernatants and biological fluids." Curr Protoc Cell Biol Chapter 3: Unit 3 22.

Thery, C., et al. (2018). "Minimal information for studies of extracellular vesicles 2018 (MISEV2018): a position statement of the International Society for Extracellular Vesicles and update of the MISEV2014 guidelines." J Extracell Vesicles 7(1): 1535750.

Valadi, H., et al. (2007). "Exosome-mediated transfer of mRNAs and microRNAs is a novel mechanism of genetic exchange between cells." Nature Cell Biology 9(6): 654-U672.

van der Pol, E., et al. (2016). "Recent developments in the nomenclature, presence, isolation, detection and clinical impact of extracellular vesicles." J Thromb Haemost 14(1): 48-56.

van der Pol, E., et al. (2012). "Single vs. swarm detection of microparticles and exosomes by flow cytometry." J Thromb Haemost 10(5): 919-930.

Vojtech, L., et al. (2014). "Exosomes in human semen carry a distinctive repertoire of small non-coding RNAs with potential regulatory functions." Nucleic Acids Res 42(11): 7290-7304.

Wolf, P. (1967). "The nature and significance of platelet products in human plasma." British journal of haematology 13(3): 269-288.

Wollert, T. and J. H. Hurley (2010). "Molecular mechanism of multivesicular body biogenesis by ESCRT complexes." Nature 464(7290): 864-869.

Yoon, S. B. and J. H. Chang (2017). "Extracellular vesicles in bile: a game changer in the diagnosis of indeterminate biliary stenoses?" Hepatobiliary Surg Nutr 6(6): 408-410.

Yuan, Z., et al. (2018). "Bronchoalveolar Lavage Exosomes in Lipopolysaccharide-induced Septic Lung Injury." J Vis Exp(135).

Zaborowski, M. P., et al. (2015). "Extracellular Vesicles: Composition, Biological Relevance, and Methods of Study." Bioscience 65(8): 783-797.

Zhang, M. D., et al. (2018). "Methods and Technologies for Exosome Isolation and Characterization." Small Methods 2(9).

Zlotogorski-Hurvitz, A., et al. (2015). "Human saliva-derived exosomes: comparing methods of isolation." J Histochem Cytochem 63(3): 181-189.

Appendix

I. Complementary Figures And Tables

Complementary Table 1. Noise distribution arising from PBS readings with flow cytometry. Percentage and count are shown at each size range.

Filter	<200 nm	200-350 nm	350-750 nm	750-1000 nm	>1000 nm
A	98.56% 145,702	1.08% 1,598	0.27% 400	0.04% 56	0.05% 68
B	85.95% 17,704	9.32% 1,920	3.39% 676	0.82% 154	0.52% 93

Complementary Table 2. Average total event count and count of GFP positive events. Numbers are calculated upon the samples' solvent baseline values.

120k	Control		EGFP		A4		CD63	
Filter	A	B	A	B	A	B	A	B
Count	32,010	144,427	30,786	128,916	80,948	284,674	106,218	240,907
GFP positive count	52	-5	1,957	1,563	8,393	7,690	16,880	10,774
16k								
Count	74,588	247,262	164,701	420,967	305,997	698,714	401,434	781,170
GFP positive count	218	24	24,211	19,397	75,570	69,111	121,244	90,961
2k								
Count	22,897	82,473	48,981	128,506	92,640	219,350	92,123	180,540
GFP positive count	199	252	8,377	7,161	21,331	19,017	30,429	24,390

Complementary Table 3. Percentage of GFP positive events in *16k* and *2k* samples from flow cytometry.

16k	Control		EGFP		A4		CD63	
Filter	A	B	A	B	A	B	A	B
GFP postive %	0.29%	0.01%	14.70%	4.61%	24.70%	9.89%	30.20%	11.64%
2k								
Filter	A	B	A	B	A	B	A	B
GFP postive %	0.87%	0.31%	17.10%	5.57%	23.03%	8.67%	33.03%	13.51%

Complementary Table 4. Size distribution of GFP positive events from flow cytometry with filter B.

Sample	<200 nm	200-350 nm	350-750 nm	750-1000 nm,	>1000 nm
EGFP 120k	86%	5%	3%	2%	4%
16k	40%	41%	13%	4%	1%
2k	50%	28%	12%	3%	7%
A4 120k	87%	6%	3%	2%	2%
16k	40%	43%	13%	3%	1%
2k	55%	29%	11%	2%	3%
CD63 120k	71%	9%	12%	5%	3%
16k	39%	42%	13%	5%	1%
2k	57%	28%	11%	2%	2%

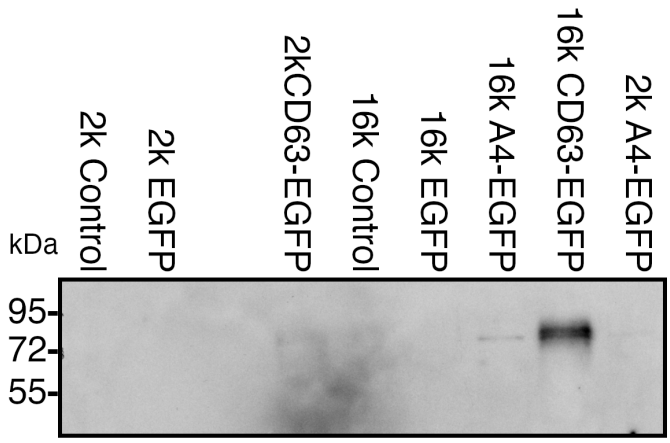

Complementary Figure 1. Blot image of the *16k* and *2k* samples. Analysis was performed with EGFP specific antibodies. Image was acquired after 30 minute exposure.

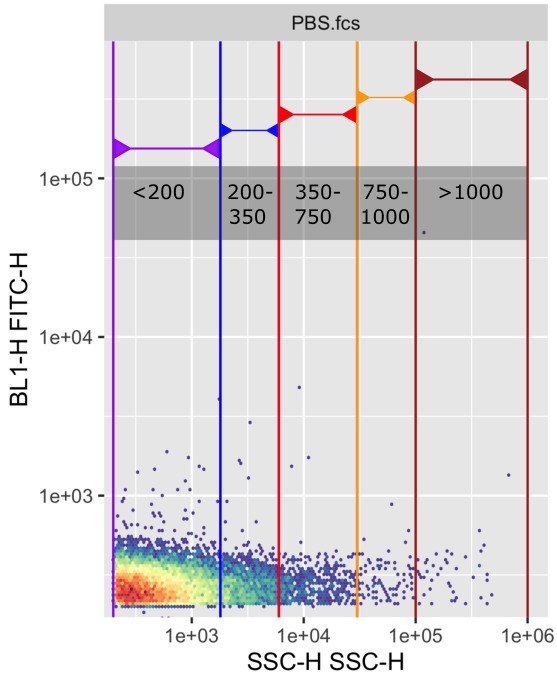

Complementary Figure 2. General schematic showing gate intervals inside dot plots of flow cytometry results. Plot is from PBS readings.